Mon. Not. R. Astron. Soc. **000**, 000–000 (2001)

The formerly X-ray reflection-dominated Seyfert 2 galaxy NGC 6300

Matteo Guainazzi[1]

[1] *XMM-Newton Science Operation Center, ESA, VILSPA, Apartado 50727, E-28080 Madrid, Spain*

8 November 2001

ABSTRACT

In this paper, a BeppoSAX observation of the bright Seyfert 2 galaxy NGC 6300 is presented. The rapidly variable emission from the active nucleus is seen through a Compton-thin ($N_H \simeq 3 \times 10^{23}$ cm^{-2}) absorber. A Compton-reflection component with an unusually high reflection fraction ($R \simeq 4.2$), and the comparison with a reflection-dominated spectrum measured by RXTE two and half years earlier suggest that NGC 6300 belongs to the class of "transient" AGN, undergoing long and repeated periods of low-activity. The spectral transition provides support to the idea that Compton-thick and Compton-thin X-ray absorbers in Seyfert 2 galaxies are decoupled, the former being most likely associated with the "torus", whereas the latter is probably located at much larger distances.

Key words: galaxies:active – galaxies:individual:NGC 6300 – galaxies:Seyfert – X-rays:galaxies

1 INTRODUCTION

The X-ray spectra of Seyfert 2 galaxies are almost always seen through a substantial photoelectric column density (Awaki et al. 1991; Turner et al. 1997a; see Pappa et al. 2001 for some recently discovered exceptions). X-ray absorbers are classified as Compton-thick or -thin, according whether their column density, N_H is larger than $\sigma_t^{-1} \simeq 1.5 \times 10^{24}$ cm^{-2}. Below 10 keV, the Active Galactic Nucleus (AGN) emission is directly visible in transmission through a Compton-thin absorber, whereas it is totally suppressed if the absorber is Compton-thick. If $N_H \lesssim 10^{25}$ cm^{-2}, high sensitivity measurements above 10 keV can still detect the transmitted emission.

Despite the above classification, the common wisdom so far has been to associate all the X-ray absorbers with the molecular, dusty "torus", which encompasses the nuclear environment in the Seyfert unification scenarios (Antonucci & Miller 1985; Antonucci 1993). However, Matt (2000) recently proposed an extension of the unification theories, where a pc-scale "torus" is responsible only for the absorption in Compton-thick objects, whereas the Compton-thin absorber should be located at much larger scales (10-100 pc), and probably associated with the host galaxy rather than with the nuclear environment. The discovery of a plethora of dusty structures in high resolution HST/WFC2 images of nearby Seyfert galaxies (Malkan et al. 1998) provides possible "optical" counterparts to the X-ray absorber*s*.

We present in this paper the results of a BeppoSAX observation of the Seyfert nucleus hosted in the moderately inclined ($\imath \simeq 51°$: Ryder et al. 1996) barred spiral galaxy NGC 6300 ($z = 0.0037$), where the combination of broad-band X-ray coverage and of a dramatic transition with respect to a Compton-thick, reflection-dominated state measured by RXTE about two and half years earlier (Leighly et al. 1999) provides valuable insights on this issue.

2 BEPPOSAX OBSERVATION AND DATA REDUCTION

BeppoSAX observed NGC 6300 from August 28 (00:41 UTC) to August 29 (16:33 UTC) 1999. In this paper, only data of the Low Energy Concentrator System (LECS, 0.5–4 keV; Parmar et al. 1997), the Medium Energy Concentrator System (MECS, 1.8-10.5 keV; Boella et al. 1997), and the Phoswitch Detector System (PDS, 13-200 keV; Frontera et al. 1997) will be presented. The data were taken from the BeppoSAX public archive. Data reduction followed standard procedures, as described, for instance, in Guainazzi et al. (1999b). Source scientific products have been extracted from circular regions of 8 and 4 radii in the LECS and MECS, respectively. Background spectra have been extracted from blank sky fields provided by the BeppoSAX Science Data Center, using the same region of the detector as the source. PDS spectra have been extracted by plain

subtraction of the spectra obtained during the 96 s-long intervals when the instrument pointed NGC 6300 and nearby $\pm 3.5^\circ$ off-axis regions. This ensures a control of the background systematics within 0.02 counts per second. Spectral rebinning ensured that each spectral bin contains at least 25 counts and that the instrumental energy resolution is oversampled by a factor not higher than 3. Cross-normalization constants have been added to all the spectral models, following the prescriptions in Fiore et al. (1999). After data screening, total exposure times were 39.5 ks, 86.2 ks and 77.2 ks for the LECS, MECS and PDS, respectively. The corresponding count rates are: $(1.18 \pm 0.07) \times 10^{-2}$ s^{-1}, $(9.91 \pm 0.11) \times 10^{-2}$ s^{-1}, and (0.70 ± 0.04) s^{-1}, respectively. The probability that the PDS detection is due to a serendipitous contaminating source is $\sim 5 \times 10^{-4}$, according to the Cagnoni et al. (1998) LogN-LogS. NGC 6300 ($l = 328^\circ$; $b = -14^\circ$) is rather close to the Galactic Ridge (GR). However, the contribution of the GR emission to the 10–60 keV flux in the $(1.3^\circ)^2$ PDS field of view is $\lesssim 5\%$ (Valinia & Marshall 1998), and is most likely totally removed in the background-subtracted spectrum by the rocking.

In this paper: errors are at 90% confidence level for one interesting parameter, and energies are quoted in the source rest frame, unless otherwise specified.

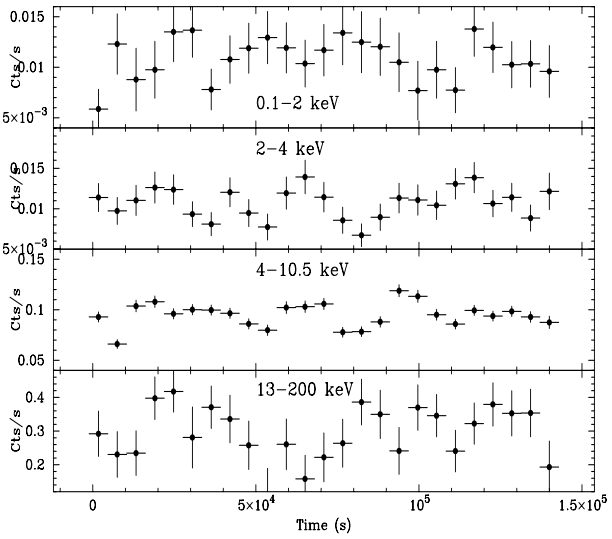

Figure 1. Light curves of the BeppoSAX observation of NGC 6300 in the 0.1–2 keV, 2–4 keV, 4–10.5 keV, and 13–200 keV energy bands (from *top* to *bottom*). The binsize is 5760 s. The curves, except the last one, are not background subtracted.

3 BEPPOSAX RESULTS

3.1 Timing analysis

In Fig. 1 we show the light curves in the 0.1–2 keV (LECS), 2–4 keV, 4–10.5 keV (MECS) and 13–200 keV (PDS) energy bands. Each bin ($\Delta t = 5760$ s) corresponds approximately to one BeppoSAX orbit. Although some variability is present in all energy bands above 2 keV, it is statistically significant only in the 4–10.5 keV band ($\chi^2_\nu = 5.4$ for 25 degrees of freedom, dof, if a constant line is fit to the data), where the statistics is the best. The X-ray flux in this band is actually variable on time scales as low as $\sim 10^3$ s (Fig. 2). The sharpest variation is a factor of 2 "flare" of about 2 ks duration, starting 110000 seconds after the beginning of the observation. No significant spectral variability is nonetheless observed. Fitting a constant line to the hardness ratio versus 4–10.5 keV count rate functions yields $\chi^2_\nu = 0.85$ and 1.35 for the 4–10.5 keV/2–4 keV and 13–200 keV/4–10.5 keV bands, respectively.

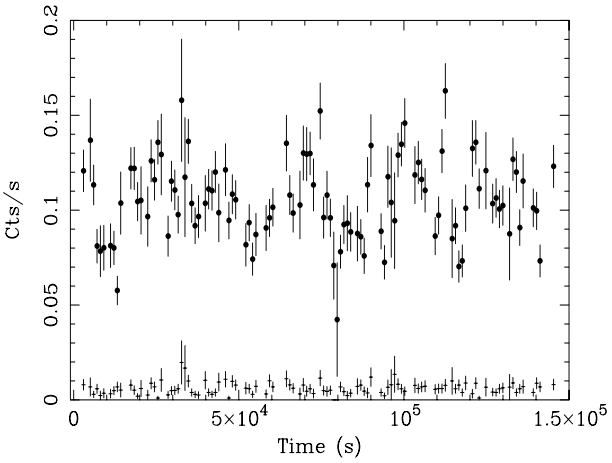

Figure 2. MECS light curve of the BeppoSAX observation of NGC 6300 in the 4–10.5 keV energy band. The binsize is 1024 s. Both the source+background (*dots*) and the background light curve (taken from a source-free region nearby NGC 6300; *crosses*) are shown

3.2 Spectral analysis

In Fig. 3 we show the BeppoSAX spectrum and the residuals against a power-law fit with photoelectric absorption. Several features are evident, and explain the bad fit ($\chi^2 = 385.7/89$ dof). The MECS spectrum exhibits a low-energy cut-off, due to a column density of a few 10^{23} cm^{-2}. This absorbed power-law will be referred to as *Compton-thin power-law* hereinafter. Both above 10 keV and below 2 keV excess emission is present. The high-energy excess cannot be ascribed to instrumental effects. The ratio between the 15–200 keV PDS flux and the extrapolation of the MECS flux in the same energy band is 1.43 ± 0.17, well above the cross-calibration normalization factor between the two instruments (0.80-0.90; Fiore et al. 1999). Additional local features

Model	Γ	N_H^{thin} (10^{23} cm^{-2})	N_H^{thick}/R (10^{23} cm^{-2})/	E_k (keV)	I_c (10^{-5} cm^{-2} s^{-1})	Γ_{soft}	χ^2/dof
1	$2.39\pm^{0.10}_{0.14}$	3.1 ± 0.2	$31\pm^{14}_{4}$	...	...	$4.4\pm^{0.5}_{0.4}$	110.6/83
2	$2.32\pm^{0.12}_{0.13}$	2.9 ± 0.2	$30\pm^{8}_{5}$	$6.27\pm^{0.13}_{0.16}$	$4.8\pm^{1.8}_{1.9}$	$4.5\pm^{0.4}_{0.3}$	87.8/81
3	$2.19\pm^{0.13}_{0.07}$	2.10 ± 0.10	$4.2\pm^{2.6}_{1.7}$	$6.21\pm^{0.15}_{0.20}$	3.6 ± 1.7	$4.7\pm^{0.5}_{0.4}$	84.3/82

Table 1. Best-fit parameters and results for the BeppoSAX observation of NGC 6300. Explanation of the models is in text

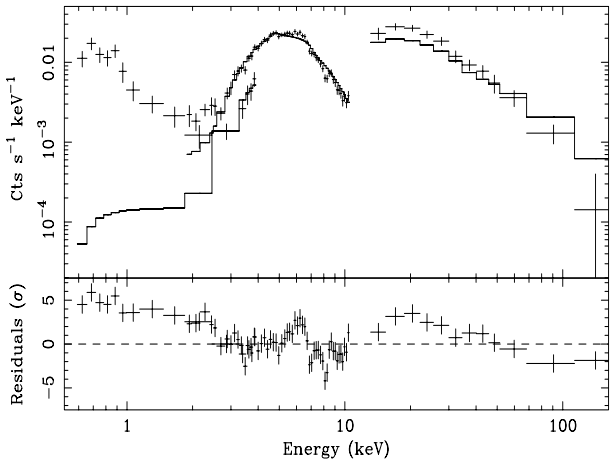

Figure 3. NGC 6300 BeppoSAX spectra (*upper panel*) and residuals in units of standard deviations (*lower panel*) when a power-law model with photoelectric absorption is applied.

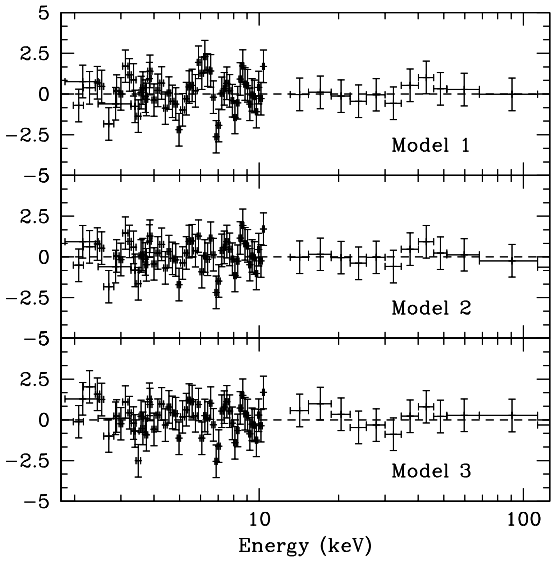

Figure 4. 2–100 keV residuals in units of standard deviations when different models are applied to the broadband BeppoSAX spectra of NGC 6300. The models are explained in text.

in the 6–8 keV range suggest the presence of either fluorescent iron emission lines or photoelectric absorption edges. A very steep ($\Gamma_{soft} \simeq 4.5$) power-law absorbed only by the column density due to our Galaxy ($N_{H,Gal} = 9.4 \times 10^{20}$ cm^{-2}; Dickey & Lockman 1990), removes the soft excess. In all the following results we make use of this model. Comparably good fits are, however, obtained if the soft excess is modeled with an optically thin, collisionally excited plasma (model `mekal` in XSPEC), which may represent the contribution of gas associated with nuclear starburst emission (Buta 1987), with $kT \simeq 500$ keV, and $Z/Z_\odot \simeq 5\%$. The quality of the BeppoSAX data does not allow us to unambiguously characterize the soft X-ray emission. The hard X-ray results presented in this paper are not significantly dependent on the choice of the soft excess model.

We have first tentatively interpreted the high energy excess as the emergence of a spectral component through a thicker absorber. We have therefore introduced an additional absorbed power-law (*Compton-thick power-law* hereinafter), whose index is held fixed to the Compton-thin power-law. If the indices are left free in the fit, indistinguishable best-fit values are yielded. The quality of the fit is marginally good ($\chi^2 = 110.6/83$ dof; Model 1 in Tab. 1). A line-like feature is still present in the residuals close to 6 keV (observer's frame; see Fig. 4). Adding a narrow (*i.e.*: intrinsic width set equal to 0) Gaussian profile yields a highly significant improvement in the quality of the fit ($\Delta\chi^2 = 22.8$ for two degrees of freedom, significant at the 99.991% confidence level; Model 2 in Tab. 1). The centroid energy of the line, $E_k = 6.27\pm^{0.13}_{0.16}$ keV, is slightly redder than expected from K_α fluorescence from fully neutral iron (as already noticed by Leighly et al. 1999), but consistent within the statistical uncertainties. The Equivalent Width (EW) is 140 ± 50 eV. The column density of the thicker absorber ($N_H \simeq 3\times10^{24}$ cm^{-2}) justifies our nomenclature. The cross-section of the thick absorber includes both the photoelectric and the optically-thin Compton scattering cross-sections, the latter playing an important rôle at such column densities. The ratio between the normalizations of the Compton-thin and -thick power laws is significantly smaller than 1: $N_{thin}/N_{thick} = 2.9\pm^{1.7}_{1.9}$ %.

The hard X-ray "bump" may be also alternatively explained in terms of Compton-reflection of the primary nuclear emission. We have therefore substituted the thick-absorbed power-law with such a component (model `pexrav` in XSPEC; Magdziarz & Zdziarski 1995). We assume an inclination angle $\cos\theta = 0.86$. The quality of the fit is comparably good ($\chi^2 = 84.3/82$ dof). The amount of reflection, R (equal to 1 for reflection of an isotropically emitted radiation by a plane-parallel, semi-infinite slab) is, however, unusually high: $R = 4.2\pm^{2.6}_{1.7}$. The exponential cut-off, if left free in the fit, tends to assume the highest possible value in the given interval. The best-fit values in Tab. 1 correspond therefore to an ideal case where no cut-off is present. The 90% lower

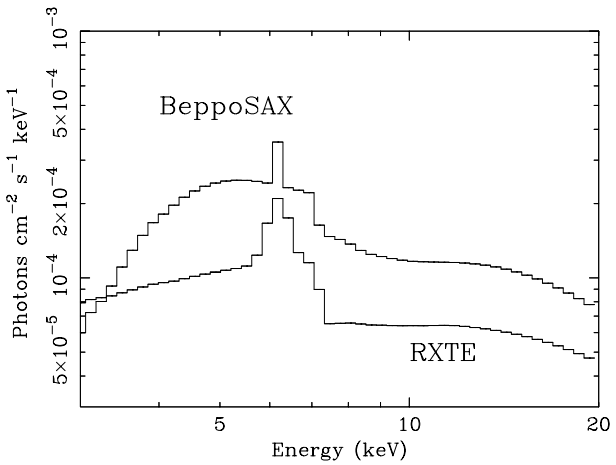

Figure 5. Best-fit models for the RXTE and BeppoSAX observations of NGC 6300.

limit on E_c is 250 keV. If $E_c = 250$ keV (1000 keV), $R \simeq 2.7$ (3.1) and $\Gamma \simeq 1.99$ (2.09). The other fit parameters are only marginally affected by the change of high-energy model. The Compton-thin column density is $N_H \simeq 2.1 \times 10^{23}$ cm^{-2}, and the equivalent width of the iron line 100 ± 50 eV.

Using Model 3 in Tab. 1, the observed fluxes are 0.12, 1.27 and 9.9×10^{-11} erg cm^{-2} s^{-1} in the 0.5–2, 2–10 and 15–200 keV energy bands, respectively. They correspond to absorption-corrected luminosities of 2.4, 1.9 and 4.9×10^{42} erg s^{-1} in the same bands, respectively.

4 COMPARISON WITH THE RXTE OBSERVATION

In Fig. 5 we compare the best fit models of the RXTE (Leighly et al. 1999) and BeppoSAX observations of NGC 6300 in the overlapping sensitive bandpass. As the former we consider the "Compton-reflection" model in Tab. 1 of Leighly et al. (1999); as the latter our Model 3 in Tab. 1. The RXTE observation caught the source in a significantly fainter and flatter state. Together with the 500-1000 eV K_α fluorescence iron line, this represents a clear signature of a Compton-reflection dominated spectrum, echo of an otherwise invisible primary continuum. The BeppoSAX spectrum is brighter in the *whole* 3–20 keV band, *i.e.* in the energy band where *both* the Compton-thin *and* the Compton-thick matter play a rôle. Interestingly enough, the intensity of the iron lines measured by RXTE and BeppoSAX is very close, and perfectly consistent within the statistical uncertainties.

5 DISCUSSION

In the 2–10 keV energy band, flux variability on timescales as short as a few 10^3 s indicates that the NGC 6300 active nucleus produces the bulk of the emission in this band. Indeed, the BeppoSAX spectrum of NGC 6300 in the same band is dominated by a standard Seyfert power-law (the intrinsic spectral index measured by BeppoSAX is slightly higher, but not extreme, among Seyfert galaxies; Turner et al. 1997a; Nandra et al. 1997), seen through a Compton-thin absorber ($N_H \simeq 2 \times 10^{23}$ cm^{-2}). This model fails, however, to account for the high-energy part of the broadband BeppoSAX spectrum, where an additional component, peaking at about 20 keV, is necessary

This component could be explained by the existence of an optical path to the nucleus, crossing a Compton-thick absorber ($N_H \simeq 10^{24}$ cm^{-2}). "Dual" or "complex" photoelectric absorbers have already been observed in intermediate (Zdziarski et al. 2001) or type 2 (Malaguti et al. 1999) Seyferts. However, this model is not in agreement with the variability in this source. The difference by a factor 30 between the normalizations of the Compton-thin and -thick power-laws in this scenario implies that the absorbing media must be decoupled*. The normalization ratio has the correct order of magnitude, if the Compton-thin power-law is actually only a fraction of the primary nuclear emission, scattered by photoionized plasma (the "warm mirror": Turner et al. 1997; Guainazzi et al. 1999a; Awaki et al. 2000; Sambruna et al. 2001) along our line of sight. However, the rapid variability observed in the 2–10 keV band would require a very small scattering region: light-crossing arguments would limit its size to $\lesssim 10^{14}$ cm. The few available variability observations suggest instead that the "warm mirrors" are located at scales $\sim$1 pc from the nucleus (Guainazzi et al. 2000), or at least at distances larger than the typical size of the Broad Line Regions (BLR; $\gtrsim 0.01$ pc) if the same matter is responsible for the broad lines components emerging in spectropolarimetric measurements of narrow-line AGN (Antonucci & Miller 1985; Tran 1995). The scattering medium must extend beyond the Compton-thick matter for the scattering optical path to be visible. Last, but not least, no evidence for iron *ionized* K_α fluorescence lines is present in the BeppoSAX data. The EW 90% upper limit are 36 eV and 16 eV for He-like and H-like iron, respectively.

A more natural explanation for the BeppoSAX spectrum is in terms of a Seyfert 1-like spectrum, seen through the Compton-thin absorber: *i.e.* a Compton-reflection component superimposed to the primary nuclear emission. However, the reflection fraction, a factor of 4 larger than typical measurements in Seyfert 1s (Nandra & Pounds 1994; Perola et al. in preparation) or Compton-thin Seyfert 2s (Turner et al. 1997), cannot be explained without a strong anisotropy of the nuclear emission or a delayed response to primary flux changes.

A clue to the origin of the reflection component may come from the long-term X-ray history of NGC 6300. The spectrum observed by BeppoSAX is dramatically different from that measured by RXTE only two and half years earlier (Leighly et al. 1999). The fainter RXTE spectrum is characterized by a very flat spectral index and a prominent ($EW \simeq$500-1000 eV) K_α fluorescence iron line. These are clear signatures of a "reflection-dominated" spectrum, *i.e.* a status where the nuclear continuum is totally disappeared or suppressed, and the bulk of the hard X-rays is due to the echo of the past nuclear activity, reflected by Compton-thick matter. In the standard Seyfert unification scenarios, the reflector is tentatively associated with the far inner side of the

* Actually this ratio is a only a lower-limit, because it does not take into account the contribution of the back-scattering by the Compton-thick absorber (Matt et al. 1999)

compact dusty molecular torus, preventing the direct view of the BLR and of the nucleus in type 2 AGN (Antonucci & Miller 1985; Antonucci 1993). If this explanation is correct (as suggested by Leighly et al. 1999), the difference with the spectral state measured by BeppoSAX is due to the later emergence of the nuclear flux.

In this scenario, there are two possible explanations for the observed spectral change. It may be due a Compton-thick absorber with $N_H > 10^{25}$ cm^{-2}, fully covering the nucleus at the time of the RXTE observation. This would have totally suppressed the Compton-thin power-law. If the Compton-thick matter in the RXTE observation was reflecting the same average flux as measured in the BeppoSAX observation, a large covering fraction is necessary to explain the RXTE "echo". Assuming that 2.5 years represents the timescale for a single homogeneous 10^{25} cm^{-2} cloud to cross the line-of-sight to the NGC 6300 nucleus, its distance from the center is $\sim 0.05 M_7^{1/3}$ pc (M_7 is the black hole mass in units of $10^7 M_\odot$). This would imply a rather peculiar geometry of the Compton-thick absorber to allow a Compton-thin optical path to be "freed" during the BeppoSAX observation.

Alternatively, NGC 6300 could represent a case of "transient" AGN, exhibiting a succession of high and low activity states. The best monitored of these transient AGN, NGC4051 (Guainazzi et al. 1998) remained in a very low state for about 100 days (Uttley et al. 1999) before returning its the normal activity. In all other known cases (Mkn 3, Iwasawa et al. 1994; NGC 2992, Gilli et al. 2000; NGC 1365, Iyomoto et al. 1997, Risaliti et al. 2001) the dimming of the X-ray flux is associated with a dramatic increase of the equivalent width of the K_α iron fluorescent line, suggesting that the delayed response of a far reprocesser is responsible for the residual X-ray flux when the primary continuum is off. In this scenario, the BeppoSAX observation represents a snapshot of the dramatic history in NGC 6300. If the covering fraction of the Compton-thick matter has not changed, the variation of the flux in the energy band where reprocessing dominates implies a factor of 4 difference in the impinging flux. Between the RXTE and the BeppoSAX observations, the AGN switched on again. However, at the time of the BeppoSAX observation the active nucleus was undergoing a new phase of *decreasing activity*, not reflected by the Compton-thick matter, which still echoed a more glorious past. A dynamical range of at least 10 in nuclear intrinsic power is necessary to explain the historical X-ray light curve of NGC 6300. The real amplitude is likely to be significant larger, our estimate being limited by the constraints on the residual amount of transmitted nuclear flux still present in the reflection-dominated state. The Compton reprocessing matter is constrained by light-travel arguments to be located within $\simeq 0.75$ pc from the nucleus. Future campaigns, monitoring the delayed response of the reprocessed spectral features, may tighten both the above estimates.

Regardless of which of the above explanations is correct, the X-ray observations of NGC 6300 have interesting implications on the nature of the X-ray absorbers in Seyfert 2 galaxies. Objects like NGC 6300 demonstrate that Compton-thin and -thick X-ray absorbers may be physically decoupled. This evidence would support to the scenarios suggested by Malkan et al. (1998) and Matt (2000), where the traditional "torus" is responsible for the Compton-thick absorbers, whereas the Compton-thin absorbers should originate at much larger distances from the nucleus, maybe associated with the host galaxy rather than with the nuclear environment. Interestingly enough, HST high-resolution images of NGC 6300 show an irregular dust distribution in the innermost 200 pc, with dusty filaments protruding (and partly covering) the active nucleus (Malkan et al. 1998).

The above results have also some implications on the origin of the iron line in Seyfert 2 galaxies. The intensity of the line in the BeppoSAX observation (corresponding to an $EW \simeq 100$–150 eV) is in principle consistent with the line being produced in transmission by a uniform Compton-thin absorber, totally encompassing the continuum source (Leahy & Creighton 1983). However, it is also perfectly consistent (within the $\simeq$30% statistical uncertainties of each individual measurement) with the intensity measured in the RXTE spectrum. This suggests that the bulk of the iron line observed in Seyfert 2s may be associated with Compton-thick matter, even when its continuum spectral signatures are not clearly visible in the 2–10 keV band, rather than to the Compton-thin absorber or to the accretion disk.

ACKNOWLEDGMENTS

Fruitful discussions with G.Matt on an early version of this manuscript are acknowledged.

REFERENCES

Antonucci R., 1993, ARA&A, 31, 473
Antonucci R.R.J., Miller J.S., 1985, ApJ, 297, 621
Awaki H., Koyama K., Inoue H., Halpern J.O., 1991, PASJ, 43, 195
Awaki H., Ueno S., Taniguchi Y., Weaver K., 2000, ApJ 542, 175
Boella G., et al., 1997, A&AS, 122, 327
Buta R., 1987, ApJS, 64, 383
Cagnoni I., Della Ceca R., Maccacaro T., 1998, ApJ, 493, 54
Dickey J.M., Lockman F.J., 1990, ARA&A, 28, 215
Fiore F., Guainazzi M., Grandi P, 1999, "Cookbook of BeppoSAX data analysis", (BeppoSAX SDC:Roma)
Frontera F., Costa E., dal Fiume D., Feroci M., Nicastro L., Orlandini M., Palazzi E., Zavattini G., 1997, A&AS, 122, 347
Gilli R., Maiolino R., Marconi A., et al., 2000, A&A, 355, 485
Guainazzi M., Nicastro F., Fiore F., et al., 1998, MNRAS, 301, L1
Guainazzi M., et al., 1999a, MNRAS, 310, 10
Guainazzi M., Molendi S., Vignati P., Matt G., Iwasawa K., 2000, NewA, 5, 235
Guainazzi M., Perola G.C., Matt G., Nicastro F., Bassani L., Fiore F., dal Fiume D., Piro L., 1999b, A&A, 346, 407
Iyomoto N., Makishima K., Fukazawa Y., Tashiro M., Ishisaki Y., 1997, PASJ, 49, 425
Iwasawa K., Yaqoob T., Awaki H., Ogasaka Y., 1994, PASJ, 46, L167
Leahy D.A., Creighton J., 1993, MNRAS, 263, 314
Leighly K.M., Halpern J.P., Awaki H., Cappi M., Ueno S., Siebert J., 1999, ApJ, 522, 209
Magdziarz P.& Zdziarski A.A., 1995, MNRAS 273, 837
Malaguti G., et al., 1999, A&A, 342, L41
Malkan M.A., Gorijn V., Tam R., 1998, ApJS, 117, 25
Matt G., 2000, A&A, 355, L13
Matt G., Pompilio F., La Franca F., 1999, NewA 4, 191
Nandra K., George I.M., Mushotzky R.F., Turner T.J., Yaqoob T., 1997, ApJ, 467, 70
Nandra K., Pounds K.A., 1994, MNRAS, 268, 405

Pappa A., Georgantopoulos I. Stewart G.C., Zezas A.L., 2001, MNRAS, in press (astro-ph 0104061)
Risaliti G., Elvis M., Nicastro F., 2001, ApJ, in press (astroph/0107510)
Ryder S.D., Buta R.J., Toledo H., Shukla H., Staveley-Smith L., Walsh W., 1996, ApJ, 460, 665
Sambruna R., Netzer H., Kaspi S., Brandt W.N., Chartas G., Garmire G.P., Nousek J.A., Weaver K.A., 2001, 546, L13
Tran H.D., 1995, ApJ, 440, 565
Turner T.J., George I.M., Nandra K., Mushotzky R.F., 1997, ApJS, 113, 23
Uttley P., McHardy I., Papadakis I.E., Guainazzi M., Fruscione A., 1999, MNRAS, 307, L6
Valinia A., Marshall F.E., 1998, ApJ, 505, 134